Journal of Dental Research
2017, Vol. 96(5) 516–523

DOI: 10.1177/0022034516689082
journals.sagepub.com/home/jdr

Decellularized Tooth Bud Scaffolds for Tooth Regeneration

W. Zhang[1], B. Vazquez[1], D. Oreadi[2], and P.C. Yelick[1]

Abstract

Whole tooth regeneration approaches currently are limited by our inability to bioengineer full-sized, living replacement teeth. Recently, decellularized organ scaffolds have shown promise for applications in regenerative medicine by providing a natural extracellular matrix environment that promotes cell attachment and tissue-specific differentiation leading to full-sized organ regeneration. We hypothesize that decellularized tooth buds (dTBs) created from unerupted porcine tooth buds (TBs) can be used to guide reseeded dental cell differentiation to form whole bioengineered teeth, thereby providing a potential off-the-shelf scaffold for whole tooth regeneration. Porcine TBs were harvested from discarded 6-mo-old pig jaws, and decellularized by successive sodium dodecyl sulfate/Triton-X cycles. Four types of replicate implants were used in this study: 1) acellular dTBs; 2) recellularized dTBs seeded with porcine dental epithelial cells, human dental pulp cells, and human umbilical vein endothelial cells (recell-dTBs); 3) dTBs seeded with bone morphogenetic protein (BMP)-2 (dTB-BMPs); and 4) freshly isolated nondecellularized natural TBs (nTBs). Replicate samples were implanted into the mandibles of host Yucatan mini-pigs and grown for 3 or 6 mo. Harvested mandibles with implanted TB constructs were fixed in formalin, decalcified, embedded in paraffin, sectioned, and analyzed via histological methods. Micro-computed tomography (CT) analysis was performed on harvested 6-mo samples prior to decalcification. All harvested constructs exhibited a high degree of cellularity. Significant production of organized dentin and enamel-like tissues was observed in dTB-recell and nTB implants, but not in dTB or dTB-BMP implants. Micro-CT analyses of 6-mo implants showed the formation of organized, bioengineered teeth of comparable size to natural teeth. To our knowledge, these results are the first to describe the potential use of dTBs for functional whole tooth regeneration.

Keywords: regenerative dentistry, postnatal dental stem cells, biomimetic scaffolds, decellularization, extracellular matrix, BMP

Introduction

Tissue engineering approaches provide promising therapeutic potential to treat congenital and acquired tissue defects. Biodegradable and biocompatible 3-dimensional (3D) scaffolds are essential for these efforts, to provide proper physical and biological cues (Griffith and Naughton 2002). Natural extracellular matrix (ECM) scaffolds are ideal candidates for tissue engineering applications (Giancotti and Ruoslahti 1999). Although fabricating biomimetic scaffolds can be challenging (Manabe et al. 2008), natural ECM scaffolds, created by gently removing immunogenic components from natural tissues or organs while preserving ECM components and architectures, can serve as superior scaffolds for tissue engineering applications. Recent reports validate the use of decellularized ECM scaffolds for a variety of tissue regeneration applications, including heart valves, nerve and blood vessels (Steinhoff et al. 2000; Funamoto et al. 2010), and also for whole organs such as the heart, liver, lung, and bladder (Ott et al. 2008; Petersen et al. 2010). Decellularized ECM scaffolds were recently approved by the US Food and Drug Administration (FDA) and have reached the commercialization stage for therapeutic applications in humans (Shitrit et al. 2014; Sicari et al. 2014).

To date, the majority of bioengineered tooth regeneration efforts have used cells/tissues isolated from embryonic tooth buds (TBs) (Ikeda et al. 2009; Oshima et al. 2011). Although these studies are highly informative, they are limited in that human embryonic TBs are not readily available. As an alternative, recent approaches have used postnatal dental cells and tissues, harvested from extracted human wisdom teeth or deciduous teeth (Young et al. 2002; Abukawa et al. 2009). This approach is also limited, in that postnatal human dental epithelial (DE) cells are not easily found, and human dental pulp (hDP)–derived stem cells alone can generate osteodentin, dentin-pulp, and periodontal ligament-like tissues, but not whole teeth (Gronthos et al. 2000; Zhang et al. 2006).

Promising research has shown that postnatal DE and dental mesenchymal (DM) cells, seeded together onto a variety of synthetic and natural scaffolds, can form very small tooth

[1]Division of Craniofacial and Molecular Genetics, Department of Orthodontics, Tufts University School of Dental Medicine, Boston, MA, USA
[2]Department of Oral and Maxillofacial Surgery, Tufts University School of Dental Medicine, Boston, MA, USA

A supplemental appendix to this article is available online.

Corresponding Author:
P.C. Yelick, Division of Craniofacial and Molecular Genetics, Department of Orthodontics, Tufts University, 136 Harrison Avenue, Room M824, Boston, MA 02111, USA.
Email: pamela.yelick@tufts.edu

crowns (Young et al. 2002; Sumita et al. 2006; Zhang et al. 2009). In contrast, the novelty of the approach described here is the use of decellularized TB (dTB) scaffolds, created from natural porcine TBs, to successfully regenerate teeth of specified size and shape. The advantage of using decellularized natural tissue scaffolds over collagen is that natural scaffolds retain many of the properties of natural tissues, thereby facilitating the differentiation of reseeded cells.

Here, we show that natural decellularized dTBs, reseeded with postnatal DE, DM, and endothelial cells, support the formation of mineralized whole teeth in an in vivo, large animal mini-pig jaw. To our knowledge, these studies are the first to demonstrate the potential use of dTB scaffolds for bioengineered tooth replacement therapies in humans.

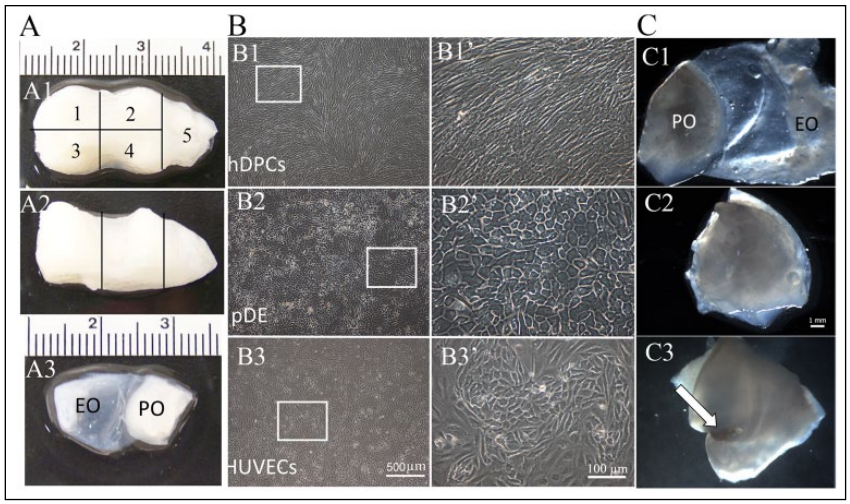

Figure 1. Recell-dTB construct preparation. (**A**) Porcine dTB. (A1, A2) Occlusal (A1) and sagittal (A2) views. (A3) Dissected dTB section. Segments 1–4 were of similar size and shape and were used for implantation. Segment 5 was used to confirm decellularization process. (**B**) Cultured cells exhibited typical cell morphologies: hDPCs (B1, B1'), pDE cells (B2, B2'), and HUVECs (B3, B3'). (B1'–B3') Higher-magnification images of boxed areas in B1 to B3. (**C**) Preparation of the recell-dTB implant. (C1) Cell-seeded dTB. (C2) EO and PO tissues were then folded together. (C3) Sutured recell-dTB construct (arrow indicates suture). dTB, decellularized tooth bud; EO, enamel organ; hDPC, human dental pulp cell; HUVEC, human umbilical vein endothelial cell; pDE, pig dental epithelial cell; PO, pulp organ.

Materials and Methods

TB Decellularization

Porcine TB decellularization was performed as we previously described (Traphagen et al. 2012). Any mineralized tooth cusps, if present, were removed after the decellularization process, prior to cell seeding.

Cell Isolation and Expansion

hDPCs and porcine DE (pDE) cells were harvested and expanded as we previously described (Young et al. 2002; Zhang et al. 2011). Human umbilical vein endothelial cells (HUVECs) were purchased from American Type Culture Collection (PSC100010; ATCC), expanded in vascular basal media (PCS100030; ATCC) with a vascular endothelial growth factor (VEGF) growth kit (PCS100041; ATCC) in 5% CO_2 at 37°C, and cryopreserved at passage 3 prior to use.

Generation of Bioengineered TB Constructs

Porcine dTBs were dissected into 5 pieces similar in size to human teeth, each of which contained enamel organ (EO) and pulp organ (PO) ECMs (Fig. 1A). Four dTB segments were used for implantation, whereas the fifth was analyzed to confirm full decellularization. Calcified cusps, when present, were carefully removed prior to use. Four construct types were analyzed: 1) acellular dTBs (four 3-mo and four 6-mo implants), 2) recell-dTBs (dTBs seeded with hDPCs, pDE cells, and HUVECs; eight 3-mo and eight 6-mo implants), 3) dTB-bone morphogenetic proteins (BMPs) (BMP-2–loaded dTBs; six 3-mo and six 6-mo implants), and 4) natural TBs (nTBs) (six 3-mo and six 6-mo implants). Each recell-dTB EO was injected with 0.5×10^6 pDE cells and 0.5×10^6 HUVECs, and recell-dTB POs were injected with 1×10^6 hDPCs and 1×10^6 HUVECs. The dental and HUVEC cell-seeding densities used in this study were selected based on our extensive published and unpublished results. Cell-seeded EO and PO were then sutured together. All constructs were cultured in a bioreactor for 1 week in 1:1:1 (DM/DE/HUVEC) media with osteogenic supplements prior to implantation.

Immunofluorescence (IF) analyses for the DE cell marker, Vimentin (sc-6260; Santa Cruz Biotechnology), the DE cell marker E-cadherin (ABIN1858334; Antibodies-Online Inc.), and the HUVEC marker Factor VIII (ab20721; Abcam) were used to confirm the survival of seeded cells prior to construct implantation. Quantification of DE cells, DM cells, and HUVECs was performed at 3 different locations within each construct using ImageJ software (National Institutes of Health). dTB-BMP constructs were injected with 5 µg of BMP-2 ~30 min before implantation. Fresh nTBs were harvested from 6-mo-old pigs 1 d prior to implantation, dissected, calcified cusps removed, and sutured together, and cultured in 1:1:1 media with osteogenic supplements overnight.

In Vivo Implantation

Animal experiments were performed using Tufts University Institutional Animal Care and Use Committee–approved protocols. The study was performed in accordance with ARRIVE (Animal Research: Reporting of In Vivo Experiments) guidelines for preclinical animal studies. Immunosuppression therapy used oral administration of prednisolone (2 mg/kg/d) and azathioprine (5 mg/kg/d) 1 d before implant placement, followed by cyclosporin (3 mg/kg/d), prednisolone (2 mg/kg/d), and azathioprine (2.5 mg/kg/d) for 2 mo (Lutton et al. 2010).

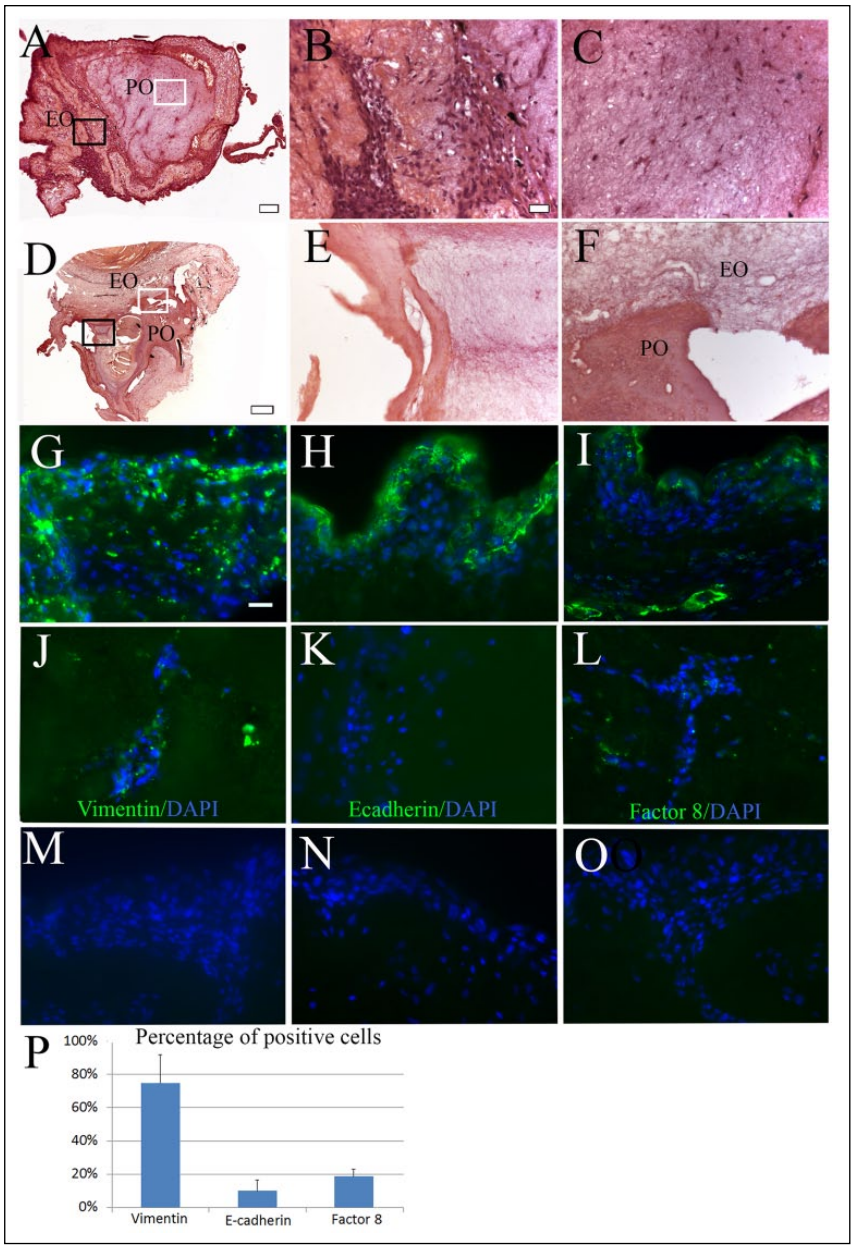

Figure 2. Recell-dTBs after 1 wk in vitro bioreactor culture. (**A**) H&E-stained sectioned recell-dTBs. (**B**, **C**) High-magnification images of black-boxed EO (B) and white-boxed PO (C) areas in A. (**D**) H&E-stained acellular dTB construct. (**E**, **F**) Higher-magnification image of black-boxed EO (E) and white-boxed PO-EO border (F) areas in D. (**G–L**) IF staining was analyzed at the periphery (G–I) and centers (J–L) of all constructs for hDPCs expressing Vimentin (G, J), pDE cells expressing E-cadherin (H, K), and HUVECs expressing Factor VIII (I, L). (**M–O**) No positive staining was observed in negative controls. (**P**) Quantitative analyses showed that ~75% of cells were positive for Vimentin, 10% cells were positive for E-cadherin, and 19% cells were positive for Factor VIII. Scale bar = 2 mm in A and D; 20 μm in B, C, E, and F to O. DAPI, 4′,6-diamidino-2-phenylindole; dTB, decellularized tooth bud; EO, enamel organ; H&E, hematoxylin and eosin; hDPC, human dental pulp cell; HUVEC, human umbilical vein endothelial cell; IF, immunofluorescence; PO, pulp organ.

Constructs were randomly implanted into curettaged fresh tooth extraction sockets of 6-mo-old Yucatan mini-pigs, 2 implants per hemimandible, and grown for 3 or 6 mo. Animals received oral antibiotics for 10 d and received a soft gel diet for 1 week postoperatively, followed by regular diet. Replicate implants were harvested using perfusion fixation, followed by an additional week of fixation in formalin.

Hard Tissue and Histological Analyses

X-rays were taken of all harvested samples, and micro-computed tomography (CT) analyses were performed on 6-mo samples using an Xradia MicroXCT-200 (Carl Zeiss X-ray Microscopy Inc.). Data reconstruction and analyses were performed using Avizo software (FEI Inc.). All samples were decalcified, embedded in paraffin, and sectioned for histological and IF analyses.

Immunohistochemical Analyses of Harvested Implants

Immunohistochemical (IHC) staining was used to identity hDP cells and HUVECs in implant constructs using anti-human mitochondria antibody (MAB1273; Millipore). Other antibodies included DM- and dentin-expressed dentin sialophosphoprotein (ab122321; Abcam) and DE- and enamel-expressed amelogenin (HPA005988; Sigma).

Results

Characterization of dTB Scaffolds

dTBs appeared white as compared to highly vascularized, reddish-colored nTBs (Appendix Fig. 1H versus A). Hematoxylin and eosin (H&E)–stained paraffin sections revealed the absence of cell nuclei, indicating complete decellularization (Appendix Fig. 1I–K), as compared to nTBs (Appendix Fig. 1B–D). Picrosirius red staining confirmed the preservation of collagen networks following decellularization (Appendix Fig. 1E–G, L–N). Please note that cusps were not removed from this sectioned specimen but were for all implanted constructs.

In Vitro Cultured TB Constructs

In vitro cultured DE cells, DM cells, and HUVECs exhibited normal morphologies (Fig. 1B1–B3, B1'–B3'). After seeding, decellularized EO and PO scaffolds retained their approximate size and shape (Fig. 1C1–C3). After 1 week in in vitro bioreactor culture, cells were easily identified throughout paraffin-sectioned recell-dTBs (Fig. 2A–C)

and were not detectable in in vitro cultured acellular dTBs (Fig. 2D–F). IF analyses were used to identify all 3 cell types (hDPCs, pDE cells, and HUVECs) in 1-week in vitro cultured recell-dTBs (Fig. 2G–L). The majority of cells were Vimentin positive (Fig. 2G, J). E-cadherin–positive DE cells were localized to the periphery of the construct (Fig. 2H versus K). Factor VIII–positive HUVECs were detected throughout the EO and PO of in vitro cultured constructs (Fig. 2I, L). Cell quantification analyses showed that in vitro cultured recell-dTB constructs consisted of ~75% hDPCs, 10% DE cells, and 19% HUVECs (Fig. 2P).

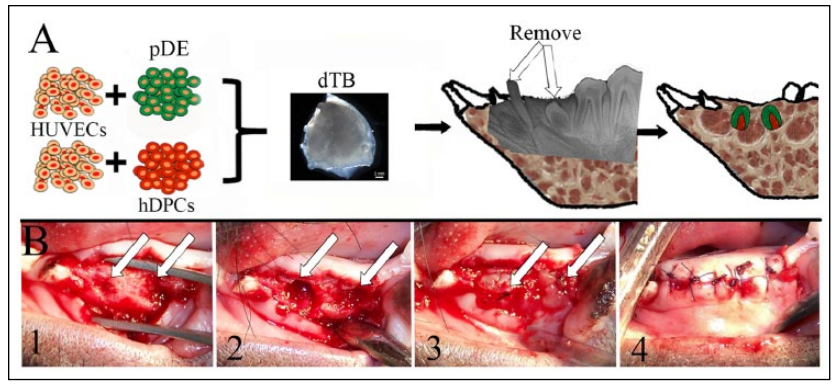

Figure 3. dTB construct implantation. (**A**) Schematic of implantation procedure. (**B**) Implant placement. (B1) Tooth extraction. (B2) Socket preparation. (B3) Implant placement. (B4) Incision closure. Arrows indicate implant sites. dTB, decellularized tooth bud; hDPC, human dental pulp cell; HUVEC, human umbilical vein endothelial cell; pDE, pig dental epithelial cell.

In Vivo Mandibular Implantation

A 6-mo-old mini-pig mandible implant model was selected for this study due to the similar size and anatomy as human mandibles (Fig. 3). Deciduous canine and first premolar teeth were removed, along with any visible replacement TBs, without any root breakage. Tooth sockets were prepared, and 2 of the same types of constructs were placed in each. All mucosal wounds healed within 7 d of implant surgery.

Implanted Construct Harvest

We obtained bright-field and X-ray images of harvested 3- and 6-mo mandibles (Appendix Fig. 2). Harvested 6-mo mandibles were larger than harvested 3-mo jaws and exhibited more permanent tooth eruption.

Characterization of In Vivo Grown Bioengineered Tooth Constructs

Histological analyses of 3-mo recell-dTB implants revealed the formation of whole tooth crowns consisting of mature enamel, dentin, and pulp in 2 of 8 implants (Fig. 4A1, A2). Bioengineered recell-dTB pulp tissues appeared highly cellularized and vascularized (Fig. 4A1, A1”, A2). Bioengineered recell-dTB teeth largely retained the original size of the dTB construct, with some distortion (Fig. 4A1, A2). Although mature tooth roots were not observed, early epithelial root sheath-like structures were identified (Fig. 4A1’ versus natural tooth epithelial root sheath in A1”). Dentin and pulp tissues were identified in 3-mo recell-dTB and nTB constructs (Fig. 4A–A2’, B–B1’).

After 6 mo of implantation, bioengineered recell-dTB teeth appeared more mature. Micro-CT analyses identified a 6-mo nTB construct consisting of a well-developed tooth crown and root (Fig. 4D–D1”; Appendix Video 1). Although no other mineralized 6-mo tooth constructs were detectable by micro-CT, paraffin-embedded and sectioned 6-mo recell-dTB constructs exhibited well-organized dentin, dental pulp, cementum, and periodontal ligament (Fig. 4E1–E1”, white boxes; Appendix Video 2).

The retention of human cells (hDPCs, HUVECs) in bioengineered tooth constructs was analyzed via human mitochondria antibody IF. Although human cells were easily detected in cultured recell-dTB constructs (Fig. 5A), very few were identified in 3-mo implants (Fig. 5B), and none were detectable in 6-mo recell-dTB implants (data not shown). Significant dentin (Fig. 5C) and enamel (Fig. 5D) tissue formation was observed in recell-dTB–derived bioengineered teeth at 3 and 6 mo. In contrast, dTB constructs appeared cellularized and formed dentin but did not exhibit enamel formation after 3- or 6-mo implantation. Control nTBs also formed new dentin but not enamel.

Discussion

Ideal tissue engineering scaffolds are biocompatible, biodegradable, and direct proper cell adhesion, migration, proliferation, and differentiation into the target tissue. As use of decellularized scaffolds has grown in popularity, decellularization methods have tailored to preserve tissue-type specific ECMs (Guyette et al. 2014). Previously, our laboratory published methods to generate dTB ECM scaffolds that supported in vitro cultured DE and DM cell attachment and proliferation (Traphagen et al. 2012). These studies identified the gentlest approach to completely decellularize porcine TBs, while retaining nTB ECM gradients. To further these studies, here we characterized in vivo implanted recell-dTB scaffolds in a mini-pig mandible model. Based on published reports using decellularized organs for regenerative medicine, we hypothesized that DE cells seeded onto decellularized EOs would be directed to form organized tooth cusps, and that DM cells seeded onto decellularized PO scaffolds would form organized dentin, pulp, and tooth root structures. As such, dTB scaffolds would direct the formation of teeth of specified size and shape. In fact, this is what we observed, in that regenerated teeth adopted the size and shape of the dTB scaffold. Our results showed the successful formation of recell-dTB–derived bioengineered whole teeth, consisting of mature enamel, pulp, dentin, periodontal ligament, and tooth roots, which adopted the size and

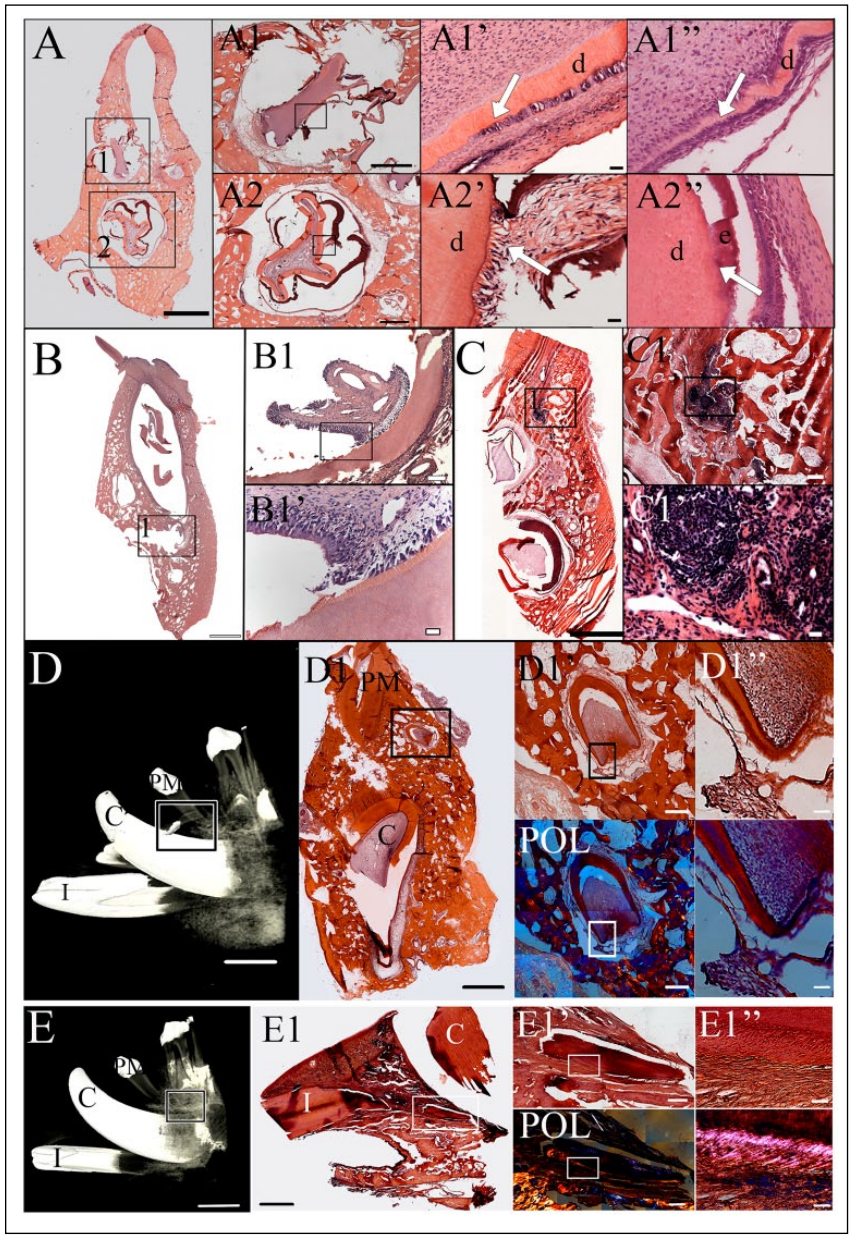

Figure 4. Histological analysis. (**A**) The recell-dTB tooth exhibited calcified enamel and dentin after 3-mo implantation. (A1, A2) High-magnification images of regenerated crowns shown in boxed areas 1 and 2 of A. (A1', A2') High-magnification images of the boxed areas of A1 and A2, respectively. The arrow in A1' indicates an epithelial root sheath-like structure similar to that of the natural tooth (A1''). (A2') Abnormal enamel-dentin junction as compared to natural teeth (A2''). (**B**) Dentin-pulp complex in a nTB sample after 3-mo implantation. (B1) Higher-magnification image of the boxed area in B. (B1') High-magnification image of the boxed area in B1. (**C**) Necrotic tissue in a dTB sample. (C1) High-magnification image of the boxed area of C. (C1') High-magnification image of the boxed area of C1. (**D**) Micro-CT image of well-developed 6-mo implanted nTB (box). (D1) H&E-stained coronal histological section of nTB crown (black box). (D1') High-magnification image of the boxed area in D1. (D1'') High-magnification image of the boxed area in D1'. POL indicates polarized light images of D1' and D1''. (**E**) Micro-CT image of a 6-mo recell-dTB implant. Although calcified structures were not detected by micro-CT, a tooth root structure was identified in sagittal histological section (E1, white box). Typical dentin and periodontal ligament-like tissues were identified under bright-field and polarized light (E1', E1''). Scale bar = 10 mm in D and E; 2 mm in A–C, D1, and E1; 500 µm in D1' and E1'; 100 µm in A1–A2, B1, and C1; and 20 µm in A1'–A2', B1', C1', D1'', and E1''. C, canal; CT, computed tomography; d, dentin; dTB, decellularized tooth bud; e, enamel; H&E, hematoxylin and eosin; I, incisor; nTB, natural tooth bud; PM, premolar; POL, polarized light.

shape of the dTB scaffold. These results demonstrate, for the first time, that dTB ECMs are capable of directing whole tooth regeneration.

It is also important to mention that not all recell-dTB constructs formed mature teeth. This observed variability in our model emphasizes the need to further refine our methods in order to reproducibly create bioengineered teeth. For example, a modified decellularization protocol, perhaps employing hydrostatic pressure (Guyette et al. 2014), may improve the quality of our dTB ECM scaffolds. Although acellular decellularized ECMs have been shown to be useful for tissue regeneration (Yates et al. 2005; Brown et al. 2010), we failed to observe tooth-like structure regeneration in our 3- or 6-mo implanted acellular dTB scaffolds. Therefore, identifying appropriate cell sources is an important consideration for successful tooth regeneration efforts. Selected cells must exhibit appropriate differentiation when seeded onto dTB ECMs, as well as the capacity to remodel immature ECM into mature tooth ECM to support functional tooth development.

This study used DE cells isolated from porcine TB and DM cells harvested from hDPs, both of which have been well characterized by us for their utility in tooth regeneration (Honda et al. 2006; Abukawa et al. 2009; Zhang W. et al. 2017). We also chose to include HUVECs based on their ability to improve vascularized tissue regeneration. Many reports show that HUVECs support the formation of neovasculature that contributes to the integration of host vasculature with implanted constructs (Zhang Q. et al. 2017), and recent studies from this laboratory showing that in vivo implanted hydrogel encapsulated DE cells, DM cells, and HUVECs supported integration with host vasculature, as well as hard and soft and dental tissue formation (Smith et al. 2017). Although abundant human cells were detected in in vitro cultured recell-dTBs prior to implantation, only a few were identified in 3-mo recell-dTB implants, and none were detected in any 6-mo implants. These results are consistent with previous publications showing that although implanted human cells do not exhibit long-term survival, they

significantly contribute to enhanced tissue regeneration (Dupont et al. 2010).

The dTBs used in this study were generated from unerupted porcine bell-stage teeth, some of which exhibited thin layers of calcified enamel and dentin at tooth cusp tips. We carefully removed any mineralized cusps from the dTB, prior to cell seeding and implantation. Despite the fact that dTBs contained no mineralized tissues, 3- and 6-mo in vivo implanted recell-dTBs exhibited calcified tooth crowns consisting of dentin and enamel. We also found that recell-dTBs and nTBs implanted for 6 mo exhibited mature calcified tooth crowns and root-like structures, whereas acellular dTB and BMP-2 implants did not.

We chose to use BMP-2 in this study based on the fact that BMP-2 has received FDA approval for bone regeneration (Ong et al. 2010) and has been shown to promote dentin formation (Wang et al. 2016). The fact that we found no calcified dental tissue formation in any BMP-2–loaded dTB implants emphasizes the importance of added cells for tooth regeneration in this model. This conclusion is also supported by the fact that recell-dTB implants exhibited more mature tooth development as compared to acellular dTB constructs.

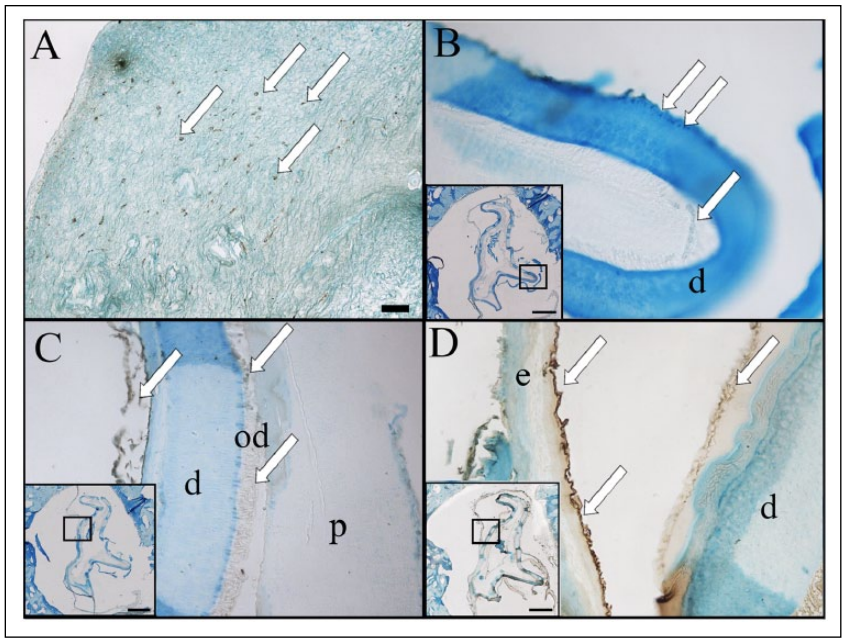

Figure 5. Immunohistochemical analysis. (**A**) Human mitochondria-positive cells were identified in an in vitro cultured recell-dTB construct. (**B**) Only a few human cells were detected in 3-mo recell-dTB implants. (**C**) Regenerated dentin exhibited positive dentin sialophosphoprotein expression (arrows). (**D**) Regenerated enamel exhibited positive amelogenin expression (arrows). Scale bar = 50 µm in A to D; 1 mm in the boxed areas in B to D. d, dentin; dTB, decellularized tooth bud; e, enamel; od, odontoblast.

Intact vascular networks benefit bioengineered construct survival by providing nutrients and facilitating efficient distribution of host progenitor cells throughout the scaffold. Since the TBs used in this study exhibited relatively immature vasculature, we used a cell injection approach to distribute both dental cells and HUVECs throughout the dTB scaffold. Subsequent histological and IHC analyses confirmed the distribution of all 3 cell types throughout recell-dTB constructs after 1 week in in vitro culture, although at densities much lower than those of nTBs. After 3- and 6-mo implantation, recell-dTBs exhibited high pulp cellularity similar to that of natural dental pulp.

Although tissue engineering methods were first published over 30 y ago (Langer and Vacanti 1993), successful whole organ regeneration remains hampered by the lack of sufficiently sophisticated, tissue-specific scaffolds (Scarritt et al. 2015). Xenotransplantation approaches in humans using decellularized porcine organs may provide a solution to this problem (Park and Woo 2012). The porcine TBs used in this study, which were harvested from slaughterhouse tissues that normally are discarded, could provide a rich source of TBs for regenerative dental applications in humans.

It is noteworthy that necrotic tissues were identified in recell-dTB, dTB, and nTB implants (Appendix Table 1), likely reflecting insufficient functional vasculature to support implant revitalization. Future modifications including the addition of angiogenic growth factors such as VEGF may improve this outcome. Although minimal immune reaction to decellularized tissues has been found (Wiles et al. 2016), damage-associated molecular pattern proteins and major histocompatibility complexes I and II can evoke immune responses that can deleteriously affect implant survival (Daly et al. 2012; Haykal et al. 2013). The fact that we observed necrotic tissues in both cellularized and acellular dTBs suggests that the observed necrosis is not caused by the seeded xenogeneic cells alone. Although the reason for the observed necrosis is unclear, the observation that necrotic tissues were detected in some of each construct type except for the dTB plus BMP constructs suggests that the addition of growth factors such as VEGF may benefit dental implant survival.

The ability to regenerate teeth of predetermined size and shape is an important goal and a major challenge for whole tooth tissue engineering efforts. Because tooth shape is normally defined in early embryonic development (Thesleff 2003; Dong et al. 2011), we wanted to determine whether exogenous cells could repopulate dTB scaffolds and form cusps to fit the dTB scaffolds. In fact, our results are highly significant, in that we found that recell-dTBs formed calcified crowns that were guided by dTB scaffolds.

Another important experimental consideration is the age of the host. In this study, 5- to 6-mo-old pig hosts were used, based on the well-documented regenerative potential of young animals (Zhang et al. 2009). However, 5- to 6-mo-old pigs have not completed supernumerary tooth development, which could potentially dislodge our implants. In fact, we found that all of the necrotic implants identified in this study were located

close to the gingiva, far from the implant site, suggesting that they were displaced toward the oral cavity during successive tooth eruption. In the future, the use of older animal hosts with adult dentition will be used to avoid this issue.

Micro-CT analysis of implants was used to identify calcified dental tissues, and histological analyses were used to characterize demineralized and soft dental tissues. These combined approaches are necessary, in that histological analyses of 6-mo bioengineered implants identified immature calcified tooth-like structures that were not detected by micro-CT (Raj et al. 2014).

In conclusion, the results and novelty of this study demonstrate, for the first time, the possibility for whole tooth regeneration using decellularized natural porcine TBs. Importantly, we showed that some of our in vivo implanted cell-seeded dTBs formed well-developed, mineralized teeth. Therefore, compared to other commonly used bioengineered scaffolds, dTBs show great potential for dental tissue regeneration, together with the fact that an ample supply of porcine TBs can be harvested from otherwise-discarded pig jaws. Limitations to this study include the fact that not all recellularized dTBs supported tooth regeneration. Regardless, these substantial and promising results indicate that further refinement of this novel approach may eventually lead to clinically relevant therapies for human tooth regeneration.

Author Contributions

W. Zhang, contributed to conception, design, data acquisition, analysis, and interpretation, drafted the manuscript; B. Vasquez, contributed to data acquisition and analysis, drafted and critically revised the manuscript; D. Oreadi, contributed to design and data acquisition, drafted and critically revised the manuscript; P.C. Yelick, contributed to conception, design, data acquisition, analysis, and interpretation, critically revised the manuscript. All authors gave final approval and agree to be accountable for all aspects of the work.

Acknowledgments

The authors thank Matthew Manning of the Yelick Laboratory and visiting scientists Arthur Gobin and Pierre-Nadim Misleh for expert technical assistance. They also thank Frances S. Brown (Tufts Cummings School of Veterinary Medicine) for expertise in paraffin sectioning and histological analyses and John Raymond Martin (Harvard School of Dental Medicine) for expert micro-CT data collection and reconstruction. This research was supported by the National Institutes of Health National Institute of Dental and Craniofacial Research (R01-DE016132 to P.C.Y.). The authors declare no potential conflicts of interest with respect to the authorship and/or publication of this article.

References

Abukawa H, Zhang W, Young CS, Asrican R, Vacanti JP, Kaban LB, Troulis MJ, Yelick PC. 2009. Reconstructing mandibular defects using autologous tissue-engineered tooth and bone constructs. J Oral Maxillofac Surg. 67(2):335–347.

Brown JW, Elkins RC, Clarke DR, Tweddell JS, Huddleston CB, Doty JR, Fehrenbacher JW, Takkenberg JJ. 2010. Performance of the CryoValve SG human decellularized pulmonary valve in 342 patients relative to the conventional CryoValve at a mean follow-up of four years. J Thorac Cardiovasc Surg. 139(2):339–348.

Daly KA, Liu S, Agrawal V, Brown BN, Johnson SA, Medberry CJ, Badylak SF. 2012. Damage associated molecular patterns within xenogeneic biologic scaffolds and their effects on host remodeling. Biomaterials. 33(1):91–101.

Dong Q, Wu H, Dong G, Lou B, Yang L, Zhang L. 2011. The morphology and mineralization of dental hard tissue in the offspring of passive smoking rats. Arch Oral Biol. 56(10):1005–1013.

Dupont KM, Sharma K, Stevens HY, Boerckel JD, Garcia AJ, Guldberg RE. 2010. Human stem cell delivery for treatment of large segmental bone defects. Proc Natl Acad Sci U S A. 107(8):3305–3310.

Funamoto S, Nam K, Kimura T, Murakoshi A, Hashimoto Y, Niwaya K, Kitamura S, Fujisato T, Kishida A. 2010. The use of high-hydrostatic pressure treatment to decellularize blood vessels. Biomaterials. 31(13):3590–3595.

Giancotti FG, Ruoslahti E. 1999. Integrin signaling. Science. 285(5430):1028–1032.

Griffith LG, Naughton G. 2002. Tissue engineering–current challenges and expanding opportunities. Science. 295(5557):1009–1014.

Gronthos S, Mankani M, Brahim J, Robey PG, Shi S. 2000. Postnatal human dental pulp stem cells (DPSCs) in vitro and in vivo. Proc Natl Acad Sci U S A. 97(25):13625–13630.

Guyette JP, Gilpin SE, Charest JM, Tapias LF, Ren X, Ott HC. 2014. Perfusion decellularization of whole organs. Nat Protoc. 9(6):1451–1468.

Haykal S, Zhou Y, Marcus P, Salna M, Machuca T, Hofer SO, Waddell TK. 2013. The effect of decellularization of tracheal allografts on leukocyte infiltration and of recellularization on regulatory T cell recruitment. Biomaterials. 34(23):5821–5832.

Honda MJ, Ohara T, Sumita Y, Ogaeri T, Kagami H, Ueda M. 2006. Preliminary study of tissue-engineered odontogenesis in the canine jaw. J Oral Maxillofac Surg. 64(2):283–289.

Ikeda E, Morita R, Nakao K, Ishida K, Nakamura T, Takano-Yamamoto T, Ogawa M, Mizuno M, Kasugai S, Tsuji T. 2009. Fully functional bioengineered tooth replacement as an organ replacement therapy. Proc Natl Acad Sci U S A. 106(32):13475–13480.

Langer R, Vacanti JP. 1993. Tissue engineering. Science. 260(5110):920–926.

Lutton BV, Cho PS, Hirsh EL, Ferguson KK, Teague AG, Hanekamp JS, Chi N, Goldman SN, Messina DJ, Houser S, et al. 2010. Approaches to avoid immune responses induced by repeated subcutaneous injections of allogeneic umbilical cord tissue-derived cells. Transplantation. 90(5):494–501.

Manabe R, Tsutsui K, Yamada T, Kimura M, Nakano I, Shimono C, Sanzen N, Furutani Y, Fukuda T, Oguri Y, et al. 2008. Transcriptome-based systematic identification of extracellular matrix proteins. Proc Natl Acad Sci U S A. 105(35):12849–12854.

Ong KL, Villarraga ML, Lau E, Carreon LY, Kurtz SM, Glassman SD. 2010. Off-label use of bone morphogenetic proteins in the United States using administrative data. Spine (Phila Pa 1976). 35(19):1794–1800.

Oshima M, Mizuno M, Imamura A, Ogawa M, Yasukawa M, Yamazaki H, Morita R, Ikeda E, Nakao K, Takano-Yamamoto T, et al. 2011. Functional tooth regeneration using a bioengineered tooth unit as a mature organ replacement regenerative therapy. PLoS One. 6(7):e21531.

Ott HC, Matthiesen TS, Goh SK, Black LD, Kren SM, Netoff TI, Taylor DA. 2008. Perfusion-decellularized matrix: using nature's platform to engineer a bioartificial heart. Nat Med. 14(2):213–221.

Park KM, Woo HM. 2012. Porcine bioengineered scaffolds as new frontiers in regenerative medicine. Transplant Proc. 44(4):1146–1150.

Petersen TH, Calle EA, Zhao L, Lee EJ, Gui L, Raredon MB, Gavrilov K, Yi T, Zhuang ZW, Breuer C, et al. 2010. Tissue-engineered lungs for in vivo implantation. Science. 329(5991):538–541.

Raj MT, Prusinkiewicz M, Cooper DM, George B, Webb MA, Boughner JC. 2014. Technique: imaging earliest tooth development in 3D using a silver-based tissue contrast agent. Anat Rec (Hoboken). 297(2):222–233.

Scarritt ME, Pashos NC, Bunnell BA. 2015. A review of cellularization strategies for tissue engineering of whole organs. Front Bioeng Biotechnol. 3:43.

Shitrit SB, Ramon Y, Bertasi G. 2014. Use of a novel acellular dermal matrix allograft to treat complex trauma wound: a case study. Int J Burns Trauma. 4(2):62–65.

Sicari BM, Rubin JP, Dearth CL, Wolf MT, Ambrosio F, Boninger M, Turner NJ, Weber DJ, Simpson TW, Wyse A, et al. 2014. An acellular biologic scaffold promotes skeletal muscle formation in mice and humans with volumetric muscle loss. Sci Transl Med. 6(234):234ra58.

Smith EE, Zhang W, Schiele NR, Khademhosseini A, Kuo CK, Yelick PC. 2017. Developing a biomimetic tooth bud model. J Tissue Eng Regen Med [epub ahead of print 8 Jan 2017] in press. doi:10.1002/term.2246

Steinhoff G, Stock U, Karim N, Mertsching H, Timke A, Meliss RR, Pethig K, Haverich A, Bader A. 2000. Tissue engineering of pulmonary heart valves on allogenic acellular matrix conduits: in vivo restoration of valve tissue. Circulation. 102(19 Suppl 3):III50–III55.

Sumita Y, Honda MJ, Ohara T, Tsuchiya S, Sagara H, Kagami H, Ueda M. 2006. Performance of collagen sponge as a 3-D scaffold for tooth-tissue engineering. Biomaterials. 27(17):3238–3248.

Thesleff I. 2003. Epithelial-mesenchymal signalling regulating tooth morphogenesis. J Cell Sci. 116(Pt 9):1647–1648.

Traphagen SB, Fourligas N, Xylas JF, Sengupta S, Kaplan DL, Georgakoudi I, Yelick PC. 2012. Characterization of natural, decellularized and reseeded porcine tooth bud matrices. Biomaterials. 33(21):5287–5296.

Wang W, Dang M, Zhang Z, Hu J, Eyster TW, Ni L, Ma PX. 2016. Dentin regeneration by stem cells of apical papilla on injectable nanofibrous microspheres and stimulated by controlled BMP-2 release. Acta Biomater. 36:63–72.

Wiles K, Fishman JM, De Coppi P, Birchall MA. 2016. The host immune response to tissue-engineered organs: current problems and future directions. Tissue Eng Part B Rev. 22(3):208–219.

Yates P, Thomson J, Galea G. 2005. Processing of whole femoral head allografts: validation methodology for the reliable removal of nucleated cells, lipid and soluble proteins using a multi-step washing procedure. Cell Tissue Bank. 6(4):277–285.

Young CS, Terada S, Vacanti JP, Honda M, Bartlett JD, Yelick PC. 2002. Tissue engineering of complex tooth structures on biodegradable polymer scaffolds. J Dent Res. 81(10):695–700.

Zhang Q, Chen ZW, Zhao YH, Liu BW, Liu NW, Ke CC, Tan HM. 2017. Bone marrow stromal cells combined with sodium ferulate and n-butylidenephthalide promote the effect of therapeutic angiogenesis via advancing astrocyte-derived trophic factors after ischemic stroke. Cell Transplant. 16;26(2):229–242.

Zhang W, Abukawa H, Troulis MJ, Kaban LB, Vacanti JP, Yelick PC. 2009. Tissue engineered hybrid tooth-bone constructs. Methods. 47(2): 122–128.

Zhang W, Ahluwalia IP, Literman R, Kaplan DL, Yelick PC. 2011. Human dental pulp progenitor cell behavior on aqueous and hexafluoroisopropanol based silk scaffolds. J Biomed Mater Res A. 97(4):414–422.

Zhang W, Vázquez B, Yelick PC. 2017. Bioengineered post-natal recombinant tooth bud models. J Tissue Eng Regen Med. 11(3):658–668.

Zhang W, Walboomers XF, van Kuppevelt TH, Daamen WF, Bian Z, Jansen JA. 2006. The performance of human dental pulp stem cells on different three-dimensional scaffold materials. Biomaterials. 27(33):5658–5668.